




Improving the Cytotoxic Activity of Hinokitiol from Drug-Loaded Phytosomal Formulation Against Breast Cancer Cell Lines

Tarek A Ahmed ^{1,2}, Ghada A Milibary¹, Alshaimaa M Almeahady¹, Amerh A Alahmadi¹, Ehab MM Ali ³, Khalid M El-Say ¹

¹Department of Pharmaceutics, Faculty of Pharmacy, King Abdulaziz University, Jeddah, 21589, Saudi Arabia; ²Centre for Artificial Intelligence in Precision Medicine, King Abdulaziz University, Alsulaymanyah, Jeddah, 21589, Saudi Arabia; ³Department of Biochemistry, Faculty of Science, King Abdulaziz University, Jeddah, 21589, Saudi Arabia

Correspondence: Tarek A Ahmed, Department of Pharmaceutics, Faculty of Pharmacy, King Abdulaziz University, Jeddah, 21589, Saudi Arabia, Tel +96626400000 ext 22250, Email tabdelnapy@kau.edu.sa

Background: This study investigates the influence of various formulation parameters on the characteristics of hinokitiol-loaded phytosomes and evaluates their anticancer potential against breast cancer cells.

Materials and Methods: Phytosomal nanoparticles were prepared and characterized for size, zeta potential, and entrapment efficiency. Morphological analysis was conducted using optical microscopy and transmission electron microscopy (TEM). The solubility of hinokitiol at different pH levels was determined, and the in vitro release profile of the optimized phytosomes was assessed. Cytotoxicity assays were performed to evaluate the anticancer efficacy against breast cancer cell lines, and apoptosis induction was examined using Annexin V/propidium iodide staining. Cell cycle analysis was conducted to assess the impact on cell cycle progression.

Results: The optimized phytosomes demonstrated a size range of 138.4 ± 7.7 to 763.7 ± 15.4 nm, with zeta potentials ranging from -10.2 ± 0.28 to -53.2 ± 1.06 mV and entrapment efficiencies between $29.161 \pm 1.163\%$ and $92.77 \pm 7.01\%$. Morphological characterization confirmed uniformity and spherical morphology. Hinokitiol solubility increased with pH, and the release from the optimized phytosomes exhibited sustained patterns. The formulated phytosomes showed superior cytotoxicity, with lower IC50 values compared to pure hinokitiol. Treatment induced significant apoptosis and cell cycle arrest at the G2/M and S phases.

Conclusion: Hinokitiol-loaded phytosomes demonstrate promising anticancer efficacy against breast cancer cells, highlighting their potential as targeted therapeutic agents for breast cancer therapy.

Keywords: hinokitiol, phytosomes, cytotoxic activity, breast cancer, apoptosis, cell cycle

Introduction

Breast cancer is a prevalent disease, impacting the lives of millions of women worldwide, making it one of the most pressing health challenges of our time. Its widespread occurrence underscores the urgent need for innovative and effective therapeutic strategies.¹ In 2020, the global burden of breast cancer was staggering, with new cases totaling 2.3 million, accounting for approximately 11.7% of all cancer incidents. Projections based on global demographic trends paint a troubling picture for the future, with anticipated cases and deaths on the rise. Trailing closely behind are lung, colorectal, prostate, and stomach cancers. Despite this shift, lung cancer remains the primary cause of cancer-related deaths, claiming an estimated 1.8 million lives. However, female breast cancer follows closely behind, underscoring the urgent need for continued research, prevention, and treatment efforts to combat this pervasive disease.^{2,3} By 2040, the worldwide burden of cancer is projected to reach 28.4 million cases, marking a significant 47% increase from the levels observed in 2020.⁴ The anticipated increase is expected to be particularly pronounced in developing nations, where projections indicate a sharp rise in prevalence from 64% to 95%. In contrast, more developed countries are expected to

see more moderate growth, from 32% to 56%. This discrepancy underscores the varying impacts of socioeconomic and healthcare infrastructure disparities between developing and developed regions. These shifts primarily stem from demographic changes, likely exacerbated by the escalating prevalence of risk factors associated with globalization and economic expansion. In light of these projections, establishing a sustainable infrastructure to disseminate cancer prevention strategies and deliver quality cancer care in transitioning countries emerges as a pivotal priority in pursuing global cancer control. The incidence of treatable cancers is increasing owing to advancements in early detection methods and the development of cutting-edge treatments. Concurrently, there is a growing global focus on preventive measures against cancer. However, as cancer treatment methodologies become increasingly intricate, the delineation of ethical standards in cancer care has become a subject of significant contention and discussion.⁵

In recent years, there has been a burgeoning interest in the potential role of herbal medicine in treating cancer. Herbal remedies, derived from various plants and natural sources, have long been utilized in traditional medicine systems across cultures worldwide.^{6,7} With the advent of modern scientific research, there has been a renewed focus on exploring the therapeutic properties of these botanical compounds in the context of cancer treatment. Herbal medicines are rich sources of bioactive compounds such as polyphenols, alkaloids, flavonoids, and terpenoids, which possess diverse pharmacological activities, including antioxidant, anti-inflammatory, and anticancer properties.⁸ While conventional cancer therapies such as chemotherapy and radiotherapy remain the cornerstone of treatment, herbal medicines are increasingly being investigated as complementary or alternative approaches to enhance efficacy, alleviate side effects, and improve overall quality of life for cancer patients.⁹ However, it is imperative to rigorously evaluate the safety, efficacy, and potential interactions of herbal remedies through robust scientific research and clinical trials to ensure their responsible integration into mainstream cancer care protocols.

Phytosomes represent an innovative approach to herbal medicine delivery that has garnered considerable attention in recent years. These novel formulations involve the complexation of phytoconstituents with phospholipids to enhance their bioavailability and therapeutic efficacy.¹⁰ By forming stable complexes with phospholipids, phytosomes overcome the limitations of poor solubility and absorption often associated with herbal extracts, thereby facilitating improved delivery and cellular uptake of bioactive compounds.¹¹ This unique lipid-based delivery system enhances the pharmacokinetic properties of herbal extracts and allows for targeted delivery to specific tissues or cells of interest. As a result, phytosomes have emerged as promising vehicles for delivering herbal medicines, offering the potential to optimize their therapeutic benefits in various clinical applications, including cancer treatment.

This study aims to investigate the potential of phytosomal formulations in enhancing the efficacy of herbal medicines, especially in cancer treatment. We focus on optimizing the formulation process to minimize the particle size and maximize the encapsulation efficiency. In vitro release studies will assess the drug release profile. Morphological characterization will ensure structural uniformity. Additionally, we will evaluate cytotoxicity against cancer cell lines and explore apoptotic and cell cycle effects. These findings aim to inform the development of targeted cancer therapeutics using phytosomal formulations.

Materials and Methods

Materials

Hinokitiol was obtained from AK Scientific (Union City, CA, USA). Phospholipon 90 G was generously provided by Lipoid GmbH (Köln, Germany). Ethanol, cholesterol, sodium deoxycholate, phosphate buffer, sodium hydroxide, potassium hydrogen phthalate, potassium dihydrogen phosphate, and sodium bicarbonate were purchased from Sigma-Aldrich (St. Louis, USA). Dulbecco's Modified Eagle's Medium (high glucose) (DMEM), fetal bovine serum (FBS), HepG2 cell cultures, and Penicillin-streptomycin 5000 U/mL antibiotics were sourced from Thermo Fisher Scientific (Waltham, MA, USA). Trypan blue, 3-(4,5-dimethylthiazol-2-yl)-2,5-diphenyltetrazolium bromide (MTT), and propidium iodide were supplied by Merck & Co Inc. (West Point, PA, USA). The Annexin V-FITC Apoptosis Kit was acquired from Creative Biolabs (Shirley, NY, USA). The MCF-7 and MDA-MB-231 cell lines were acquired from the American Type Culture Collection (Manassas, Virginia, USA).

Draper-Lin Small Composite Experimental Design

In this study, the drug-loaded phytosomal formulations were developed using the Draper-Lin small composite experimental design as suggested by the Statgraphics Centurion XV, version 15.2.05 software (StatPoint, Inc., Warrenton, VA, USA). In this study, the impact of four independent variables (X1: drug-to-phospholipid molar ratio, X2: percentage of cholesterol to total phospholipid, X3: percentage of deoxycholic acid to total phospholipid, and X4: pH of the hydration medium) on three responses (Y1: particle size, Y2: zeta potential, and Y3: entrapment efficiency) of hinokitiol phytosomes was investigated. The software recommended the Draper-Lin small composite design as an efficient and robust approach to explore the relationships between these variables and the studied responses. This design is particularly suitable for optimizing formulations with a moderate number of factors while minimizing the number of experimental runs compared to full factorial designs. The independent variables (X1-X4) and their levels were identified based on our preliminary trials and the literature review. The drug-to-phospholipid molar ratio, percentage of cholesterol to phospholipid, percentage of deoxycholic acid to phospholipid, and the pH of the hydration medium were adjusted to ranges of 1–3, 5–30, 5–20, and 5.5–9.3, respectively.

Preparation of the Hinokitiol-Loaded Phytosomal Formulations

The composition of the eighteen drug-loaded phytosomal formulations proposed by the Draper-Lin small composite experimental design is illustrated in Table 1. Formulation preparation was conducted using the thin film hydration technique as previously described in the literature.^{12–14} Briefly, the known weight of the drug (100 mg) and the calculated amount of phospholipid, cholesterol, and sodium deoxycholate were dissolved in ethanol with the aid of water bath sonication in a rounded bottom flask. Subsequently, the organic solvent (ethanol) was evaporated using a Buchi Rotavapor R-200 (Buchi labortechnik AG, CH-9230, Flawil, Switzerland) at 45°C under reduced pressure until a thin lipid film was formed inside the container. To ensure complete removal of the organic solvent, the container containing the lipid film was left overnight at 25°C in a vacuum oven from Thermo Fisher Scientific Inc. (OH, USA). Then, a known volume of the specified hydration

Table 1 Composition of the Hinokitiol-Loaded Phytosomal Formulations and the Observed Values of the Dependent Variables

| Run | Independent Variables | | | | Dependent Variables | | |
|-----|-----------------------|------|------|------|---------------------|------------|------------|
| | X1 | X2 | X3 | X4 | Y1 (nm) | Y2 (mV) | Y3 (%) |
| F1 | 1:2 | 17.5 | 12.5 | 7.4 | 595±55.6 | -41.3±0.78 | 60.35±4.05 |
| F2 | 1:2 | 17.5 | 12.5 | 7.4 | 576.1±98.2 | -41.3±0.78 | 62.44±3.33 |
| F3 | 1:2 | 17.5 | 0 | 7.4 | 695±27.4 | -10.2±0.28 | 62.93±4.32 |
| F4 | 1:2 | 38.5 | 12.5 | 7.4 | 738.4±25.3 | -40.8±1.30 | 60.36±5.09 |
| F5 | 1:3 | 30 | 20 | 5.5 | 484.6±43.2 | -35.2±1.20 | 90.63±7.06 |
| F6 | 1:1 | 30 | 5 | 9.3 | 196.6±13.2 | -40.5±0.64 | 44.17±3.09 |
| F7 | 1:3 | 5 | 20 | 9.3 | 457.3±15.0 | -49±0.50 | 53.18±3.36 |
| F8 | 1:1 | 30 | 20 | 9.3 | 138.4±7.7 | -53.2±1.06 | 43.09±3.26 |
| F9 | 1:3.68 | 17.5 | 12.5 | 7.4 | 763.7±15.4 | -42.7±0.57 | 85.25±6.29 |
| F10 | 1:1 | 5 | 20 | 5.5 | 183.2±29.3 | -31.6±0.35 | 64.55±3.26 |
| F11 | 1:0.32 | 17.5 | 12.5 | 7.4 | 191.7±3.9 | -39.4±2.69 | 41.88±1.09 |
| F12 | 1:2 | 0 | 12.5 | 7.4 | 216.7±18.1 | -41.2±0.50 | 61.81±3.16 |
| F13 | 1:1 | 5 | 5 | 5.5 | 290.9±38.4 | -27.2±0.14 | 66.31±3.09 |
| F14 | 1:2 | 17.5 | 12.5 | 10.6 | 496.2±28.3 | -50.2±0.14 | 29.16±1.16 |
| F15 | 1:2 | 17.5 | 12.5 | 4.2 | 454.2±37.8 | -18.8±0.57 | 92.77±7.01 |
| F16 | 1:2 | 17.5 | 25.1 | 7.4 | 228.4±12.9 | -45.5±0.63 | 55.14±4.31 |
| F17 | 1:3 | 5 | 5 | 9.3 | 485.3±4.5 | -40.3±0.78 | 53.79±1.06 |
| F18 | 1:3 | 30 | 5 | 5.5 | 756.9±12.3 | -18.8±0.14 | 91.94±6.07 |

Abbreviations: X1; drug-to-phospholipid molar ratio, X2; percentage of cholesterol to total phospholipid, X3; percentage of deoxycholic acid to total phospholipid, X4; pH of the hydration media, Y1; particle size, Y2; zeta potential, Y3; entrapment efficiency.

medium (50 mL) was added to the lipid film, and the mixture was stirred at 50°C for 30 minutes. Finally, the mixture was subjected to high-speed homogenization at 20,000 rpm for 10 minutes to achieve uniform dispersion.

Characterization of the Prepared Formulations

Determination of Particle Size and Zeta Potential

Particle size, polydispersity index (PDI), and zeta potential of the 18 phytosome nanoparticle formulations were determined using a Malvern Zetasizer Nano ZSP (Malvern Panalytical Ltd., Malvern, UK). Dynamic light scattering with non-invasive backscatter optics was employed to measure the average particle size and polydispersity index, while laser Doppler micro-electrophoresis was utilized for zeta potential determination. Analysis was conducted using Malvern Zetasizer software version 7.12, with triplicate measurements performed for each formulation.

Measurement of Entrapment Efficiency

An indirect estimation of the percentage of hinokitiol entrapped by the phytosome nanoparticle formulations was conducted. Phytosome nanoparticle formulations (n = 3) were centrifuged using a Sigma Laboratory centrifuge (Ostrode, Germany) at 15,000 rpm for 60 minutes in Amicon[®] falcon tubes containing a known volume of each formulation. Separation of the supernatant and filtration were performed using a 0.22 µm filter. Spectrophotometric analysis was carried out at a wavelength (λ_{max}) of 241 nm on the free drug supernatant. The supernatant of drug-free phytosomal formulation was used as a blank in the spectrophotometric analysis to avoid interference.

The following equation was utilized to calculate the entrapment efficiency (EE):

$$EE = \frac{\text{Total amount of drug used} - \text{Calculated amount of free drug in supernatant}}{\text{Total amount of drug used}} \times 100 \quad (1)$$

Draper-Lin Small Composite Experimental Design Statistical Analysis

The data for particle size, zeta potential, and entrapment efficiency (EE) were analyzed to determine the significant independent factors (main effects) influencing each response variable. This analysis was performed using StatGraphics Centurion XV version 15.2.05 software from StatPoint Technologies, Inc. (Warrenton, VA, USA). Additionally, interaction and quadratic effects among the variables were assessed, with significance determined by a p-value < 0.05. The optimized levels for variables X1, X2, X3, and X4 were identified based on the analysis. Subsequently, the optimized formulation was prepared and characterized as described above. Finally, predicted and observed values for particle size (Y1), zeta potential (Y2), and entrapment efficiency (Y3) were compared to validate the model's predictive capability.

Morphological Characterization of the Optimized Formulation

The morphological features of the optimized drug-loaded phytosomal formulation were identified using optical microscopy and transmission electron microscopy (TEM). Optical microscopy was conducted using a Leica DM300 optical microscope (Wetzlar, Germany) to provide macroscopic insights into the morphology of the phytosomal particles. This technique allows for the visualization of particle size, shape, and aggregation at a magnification suitable for observing larger structures. Additionally, high-resolution transmission electron microscopy was performed using a JEOL JEM-2100 instrument (Tokyo, Japan) to provide detailed microscopic images of the phytosomal nanoparticles at the nanoscale level. TEM enables visualization of individual nanoparticles with high resolution, allowing for the assessment of particle size distribution, shape, and surface morphology. Combined, these microscopy techniques offer comprehensive insights into the morphological characteristics of the optimized phytosomal formulation, facilitating a better understanding of its structural properties and uniformity.

Hinokitiol Solubility Study

To assess the aqueous solubility of the drug and elucidate its solubility characteristics across varying pH conditions, which may aid in understanding the drug entrapment efficiency within the prepared phytosomes, the solubility of hinokitiol was investigated using a shake-flask method. Excess hinokitiol was added to distilled water and phosphate

buffers of varying pH (4.2, 5.5, 7.4, 9.3, and 10.6). Buffer of 7.4 was selected as a midpoint, and lower and higher values compatible with the experimental design were selected. The mixtures were shaken for 48 hours at 25°C, then were removed from the shaker and set aside for one hour, the supernatant was then filtered through a 0.45 µm membrane filter, and the concentration of hinokitiol in the filtrate was determined using UV-Vis spectroscopy at the appropriate wavelength. The experiment was conducted in triplicate.

In vitro Drug Release Study

The optimized formulation's in vitro drug release profile was evaluated and compared to that of a pure drug suspension. The drug suspension was prepared by dispersing the drug in the selected hydration medium (pH 4.2) under constant stirring to ensure a uniform suspension. Five milliliters of the phytosomal formulation or the drug suspension (2 mg/mL) was placed into the dialysis bag, with both ends secured by clamps. A phosphate buffer solution with a pH of 7.4 was selected as the release medium to mimic physiological conditions. The release was performed using a dialysis bag with a molecular weight cutoff (MWCO) of 3.5 kDa and 22 mm (Thermo Fisher Scientific, Rockford, IL, USA) submerged in 100 mL of phosphate buffer medium. At predetermined time intervals, samples (1 mL) were withdrawn from the release medium with immediate replacement to maintain sink conditions. The withdrawn samples were then analyzed spectrophotometrically at a wavelength (λ_{max}) of 241 nm to quantify the drug released. This experiment was conducted in triplicate to ensure the reliability and reproducibility of the results.

Study of in vitro Cytotoxicity

Conditions of Culture and Human Cell Lines

Two human breast cancer cell lines, namely MCF-7 and MDA-MB-231, were employed to assess the anticancer efficacy of hinokitiol-loaded phytosomal formulation compared to the pure drug. In vitro cytotoxicity experiments were conducted at the Tissue Culture Unit within the Department of Biochemistry, Faculty of Science at KAU. The cells were cultured in Dulbecco's Modified Eagle's Medium (DMEM), supplemented with 1% antibiotic and 10% fetal bovine serum, for 24 hours. The DMEM was obtained from Gibco Life Technologies. Following incubation at 37°C in a 5% CO₂ atmosphere, 90% of the attached cells were removed by treatment with 4 mL of 0.25% trypsin with EDTA, followed by a 5-minute incubation in a CO₂ incubator. The trypsinization process was terminated by adding 5 mL of complete medium. After centrifugation of the medium containing the detached cells, the pellets underwent two sterile washes with phosphate-buffered saline (PBS).^{15,16} Following the staining of 20 µL of the cell-containing media with 0.4% trypan blue, the cell count was assessed using a hemocytometer, and cells were counted in the four major squares. The following equation was applied to determine the number of cells per milliliter: $(1/4) \times 10^4 \times 2$. Subsequently, a 96-well microplate was filled with 0.1 mL of 5000 cells suspended in complete media per well. The plate was then placed in the incubator and incubated for one day.

Assessment of Cell Viability

The anticancer properties of the prepared hinokitiol-loaded phytosomal formulation "test", cisplatin "positive control", pure hinokitiol "unencapsulated form", and non-medicated phytosomes "negative control" were assessed using the MTT (3-(4,5-dimethylthiazol-2-yl)-2,5-diphenyltetrazolium bromide) assay. When the cell culture reached 70% confluence, various formulation concentrations ranging from 6.25 to 100 µg/mL were applied to the media. Each concentration was tested in quadruplicate. Following 48 hours of incubation, the media in each well were substituted with 100 µL of fresh media containing 0.5 mg/mL of MTT and incubated for an additional 4 hours. Subsequently, 100 µL of dimethylsulfoxide (DMSO) was added to each well and left for 15 minutes at room temperature before absorbance readings were taken at 490 nm using a microplate reader (Bio-RAD microplate reader, Japan). The 50% inhibitory concentration (IC₅₀) of the hinokitiol-phytosomal formulation was determined using the concentration-response curve for cell viability plotted against the formulation concentration, utilizing the two respective cell lines.^{15,16} It must be mentioned that the solubility of hinokitiol in the Dulbecco's Modified Eagle's Medium was sufficient to maintain concentrations above the IC₅₀ for both MDA-MB-231 and MCF-7 cell lines, ensuring that the drug was available at effective concentrations during the assays.

Cell Apoptosis Assay

Apoptosis, often called programmed cell death, is a natural mechanism for removing abnormal cells, preventing the proliferation of potentially cancerous cells, and maintaining overall cellular integrity. Dysregulation of apoptosis is implicated in various diseases, including cancer, where evasion of apoptosis contributes to tumor development, progression, and resistance to therapy. Its study during the investigation of new anticancer formulations is essential for assessing efficacy, predicting treatment response, and optimizing therapeutic strategies.^{17,18}

Using Annexin V-FITC/propidium iodide staining, MDA-MB-231 cells treated with HK-phytosomal formulation were assessed for necrosis and apoptosis. MDA-MB-231 cells were cultured in a CO₂ incubator for 24 hours, followed by trypsinization for cell division and counting. Subsequently, 2×10^5 cells were seeded in a 6-well plate and cultured for 24 hours in complete media supplemented with the formulation's IC₅₀ concentration. After the incubation period, the MDA-MB-231 cells were detached using trypsin, and the media-containing cells from each well were collected and centrifuged. The cell pellets were then washed with phosphate-buffered saline (PBS) solution. Annexin V-FITC/propidium iodide (PI) solution (25 μ L) and 400 μ L of binding buffer were added to 100 μ L of suspended treated MDA-MB-231 cells. Flow cytometry was employed to detect the cells, and automatic calculations were performed using the software module.¹⁹

Cell Cycle Analysis Assay

The cell cycle is a series of events that occur in a cell, leading to its division and duplication. It consists of a sequence of phases, each characterized by specific events and activities that regulate cell growth, replication, and division. Dysregulation of the cell cycle is a hallmark feature of cancer, contributing to uncontrolled cell proliferation, tumor growth, and disease progression.²⁰

Cell cycle analysis is a technique used to examine the distribution of cells within different phases of the cell cycle, including G1 (gap 1), S (synthesis), G2 (gap 2), and M (mitosis). This analysis provides valuable information about a cell population's proliferative capacity, growth kinetics, and cell cycle progression. It is a powerful tool for investigating the effects of new anticancer formulations on cell proliferation, growth kinetics, and cell cycle progression. By understanding how these formulations influence cell cycle dynamics, researchers can elucidate their mechanisms of action, identify potential targets for intervention, and optimize treatment strategies for improved therapeutic outcomes in cancer patients.²¹

In this study, cell cycle analysis was conducted using propidium iodide-based flow cytometry on MDA-MB-231 cells treated with hinokitiol-phytosomal formulation. Propidium iodide (PI) staining is a well-established method for assessing cell cycle distributions via flow cytometry.²² MDA-MB-231 cells were cultured in a 6-well plate at a density of 1×10^6 cells per well and allowed to grow for 24 hours. The growth medium was replaced with a fresh medium containing the IC₅₀ concentration of hinokitiol phytosomes formulation. Following a 24-hour treatment period, 0.5 mL of 0.25% trypsin was added to each well to detach the cells, and the trypsin activity was halted by adding 0.5 mL of complete medium. The detached MDA-MB-231 cells were centrifuged at 1500 rpm for 5 minutes and washed twice with PBS. Subsequently, the cells were fixed by incubating them in 1 mL of ice-cold 70% ethanol for at least four hours at -20°C . After fixation, the cells were washed with 100 μ L of cold PBS containing RNase A and then stained with 250 μ L of PI solution (50 mg/mL PI) for one hour in the dark. Finally, flow cytometric analysis was performed on each sample using a flow cytometer (Applied Biosystems, USA).

Statistical Analysis

The results of the analysis of treated cell viability are presented as mean \pm standard deviation (SD). GraphPad Prism Software (version 9.0) was employed to determine the half-maximal inhibitory concentration (IC₅₀) of the medication and conduct statistical analyses on all collected data. Flow cytometry software determined the percentages of cells in each phase of the cell cycle and the counts of necrotic and apoptotic cells.

Results and Discussion

A series of small-scale experiments to explore the ranges of the drug-to-phospholipid molar ratio (X1), the percentage of cholesterol to phospholipid (X2), the percentage of deoxycholic acid to phospholipid (X3), and the pH of the hydration

medium (X4) were conducted as preliminary trials. These trials helped us establish the ranges of the studied independent variables. The drug-to-phospholipid molar ratio (X1) was tested in a range of 1–3, as lower ratios resulted in inadequate drug loading, while higher ratios caused aggregation and instability of the phytosomes. Initial tests for cholesterol percentage (X2) with a broader range of cholesterol content indicated that levels below 5% compromised membrane stability, while levels above 30% led to excessive rigidity, which impacted particle size and drug release. The range of 5–20% for deoxycholic acid percentage (X3) was optimal after testing a more comprehensive range, as amounts below 5% resulted in poor membrane integrity, while concentrations above 20% led to undesirable particle aggregation. A pH range of 5.5–9.3 for the hydration medium (X4) was selected based on the drug solubility that will be mentioned later. These preliminary trials were not part of the main study but were essential for selecting the factor ranges used in the Draper-Lin small composite experimental design.

Characterization and Optimization of the Prepared Phytosomal Formulations

The results depicting the observed values for particle size (Y1), zeta potential (Y2), and entrapment efficiency (Y3) are outlined in Table 1. The prepared phytosomal nanoparticles exhibited a diameter size range of 138.4 ± 7.7 to 763.7 ± 15.4 nm, zeta potential ranging from -10.2 ± 0.28 to -53.2 ± 1.06 mV, and entrapment efficiency ranging between $29.161 \pm 1.163\%$ and $92.77 \pm 7.01\%$. All formulations' polydispersity index (PDI) was within the range of 0.449 ± 0.02 to 0.848 ± 0.045 . While a PDI below 0.5 typically indicates a more uniform size distribution, values approaching 0.8 can still represent a reasonable dispersion for lipid-based nanosystems, such as phytosomes, which tend to show some heterogeneity due to their complex structure. It is recommended that, during the development of the phytosomal formulations, a detailed comparison of particle size reduction and drug loading efficiency be conducted before and after homogenization to ensure that the desired particle size is achieved without compromising drug entrapment efficiency.

Statistical analysis to assess the impact of the independent variables (X1–X4) on the studied responses (Y1–Y3) was conducted through multiple regression analysis and two-way analysis of variance using Statgraphics software. Notably, X1, X2, and X3 significantly influenced the particle size of the prepared phytosomal formulations, whereas X3 and X4 significantly affected zeta potential. Additionally, X1 and X4 significantly impacted drug entrapment efficiency, as demonstrated in the Pareto chart presented in Figure 1. A reference line indicating a P-value of 0.05 is depicted in this chart, with any factor effect surpassing this line deemed to significantly influence the studied response.

The equations of the fitted models were found to be:

$$Y1 = 506.404 - 364.447 * X1 + 23.633 * X2 + 1.84325 * X3 - 2.48454 * X4 - 47.9626 * X1^2 + 5.37891 * X1X2 - 2.24 * X1X3 + 89.2193 * X1X4 - 0.440521 * X2^2 - 0.259733 * X2X3 - 0.0765641 * X2X4 - 0.96265 * X3^2 + 2.57719 * X3X4 - 13.5309 * X4^2 \quad (2)$$

$$Y2 = 20.6581 + 2.92856 * X1 + 1.29292 * X2 - 2.05122 * X3 - 9.96392 * X4 - 0.799399 * X1^2 - 0.0448218 * X1X2 - 0.133333 * X1X3 + 0.234998 * X1X4 - 0.00665386 * X2^2 - 0.0213333 * X2X3 - 0.0897305 * X2X4 + 0.0693755 * X3^2 - 0.00526316 * X3X4 + 0.420047 * X4^2 \quad (3)$$

$$Y3 = 101.115 + 31.0427 * X1 - 0.828478 * X2 - 0.224054 * X3 - 10.1821 * X4 + 1.44531 * X1^2 - 0.32097 * X1X2 + 0.0152667 * X1X3 - 2.50035 * X1X4 + 0.00500694 * X2^2 - 0.0000213333 * X2X3 + 0.166955 * X2X4 - 0.00279529 * X3^2 + 0.0120877 * X3X4 + 0.145718 * X4^2 \quad (4)$$

The fitted model equation in statistical analysis holds significant importance as it provides a concise mathematical representation of the relationship between the independent variables and the dependent variable. The fitted model equation allows researchers to predict the value of the dependent variable (response) for given values of the independent variables. This predictive capability is valuable for forecasting outcomes and making informed decisions.

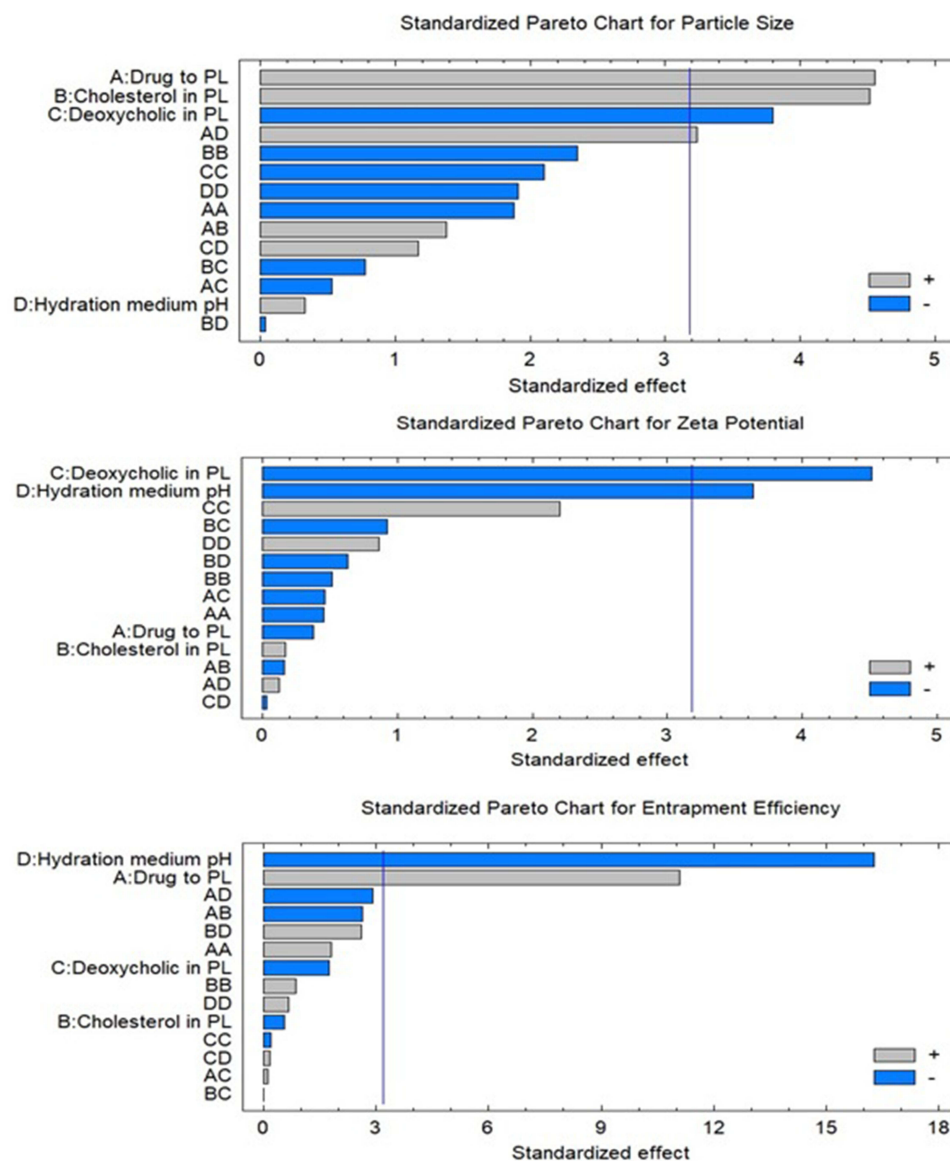


Figure 1 Standardized Pareto chart for the effect of the studied factors on particle size, zeta potential, and entrapment efficiency.

To illustrate the effect of two independent variables on a studied response when the values of the other two independent variables were kept at their intermediate levels, the response surface plots were constructed as depicted in [Figure 2](#) for the particle size, [Figure 3](#) for the zeta potential, and [Figure 4](#) for the entrapment efficiency.

The drug-to-phospholipid ratio (X1) exerted a significant positive synergistic effect on both particle size (Y1) and entrapment efficiency (Y3). This behavior is likely attributable to the formation of multilamellar vesicles of larger size with increasing X1 ratio from 1:1 to 1:3. These vesicles can accommodate or entrap a greater amount of drug between the layers, resulting in increased particle size and entrapment efficiency as previously mentioned.¹³ The percentage of cholesterol in phospholipid (X2) significantly influenced particle size, exhibiting a synergistic positive effect. Previous studies explained the role of cholesterol in enhancing the phospholipid packaging during development of lipid-based nanoparticles such as liposomes.²³ Tefas et al investigated the influence of cholesterol in liposome formulation and demonstrated that cholesterol enhances the packing of phospholipids, and decreases membrane permeability. Consequently, it imparts a more rigid structure to the lipid membrane, resulting in larger, more stable vesicles.²⁴ In lipid-based systems, including phytosomes, an increase in cholesterol content can lead to larger particles because cholesterol can disrupt the packing of phospholipids, creating a more disordered membrane structure. This disruption can cause an expansion of the lipid bilayer, resulting in an overall increase in particle size. Additionally,

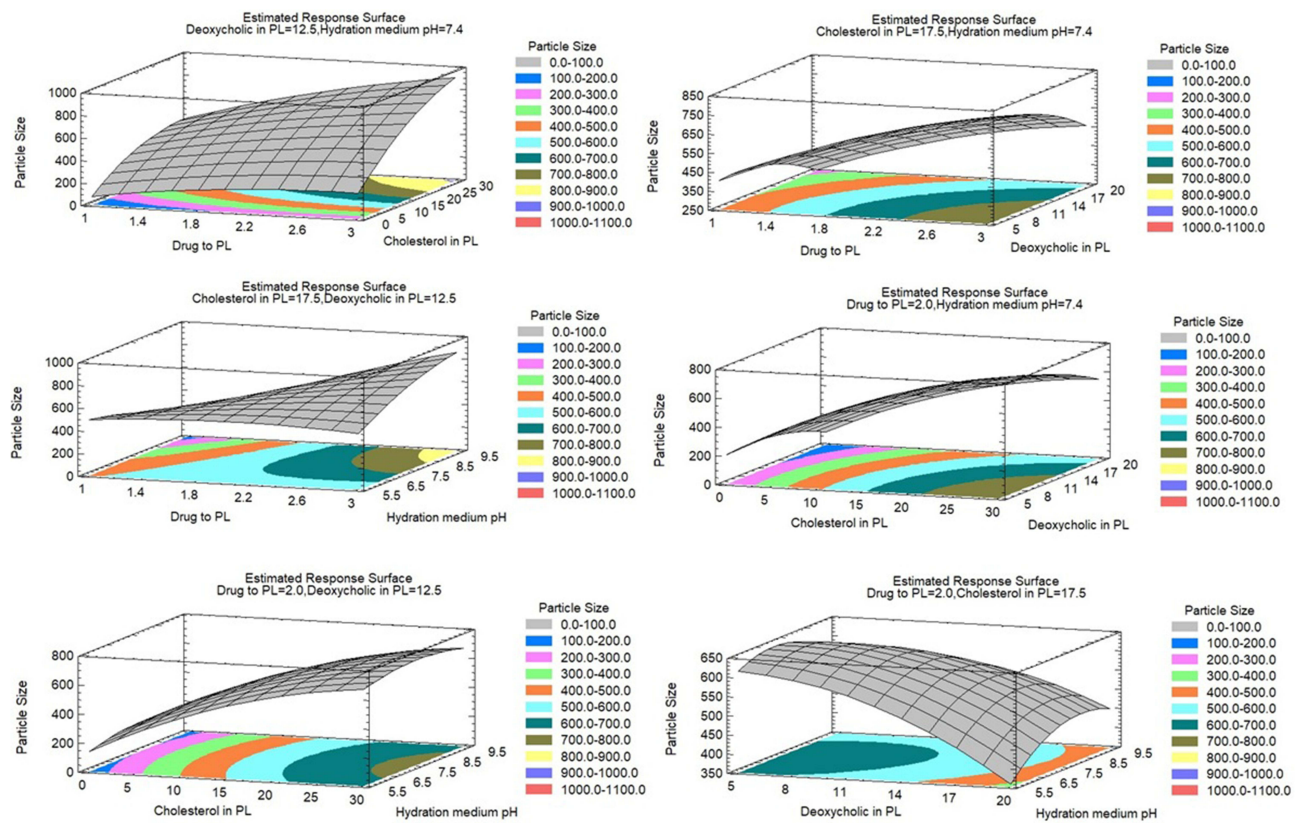


Figure 2 Estimated response surface plots for the effect of the studied factors on particle size of the prepared hinokitiol-loaded phytosomal formulations.

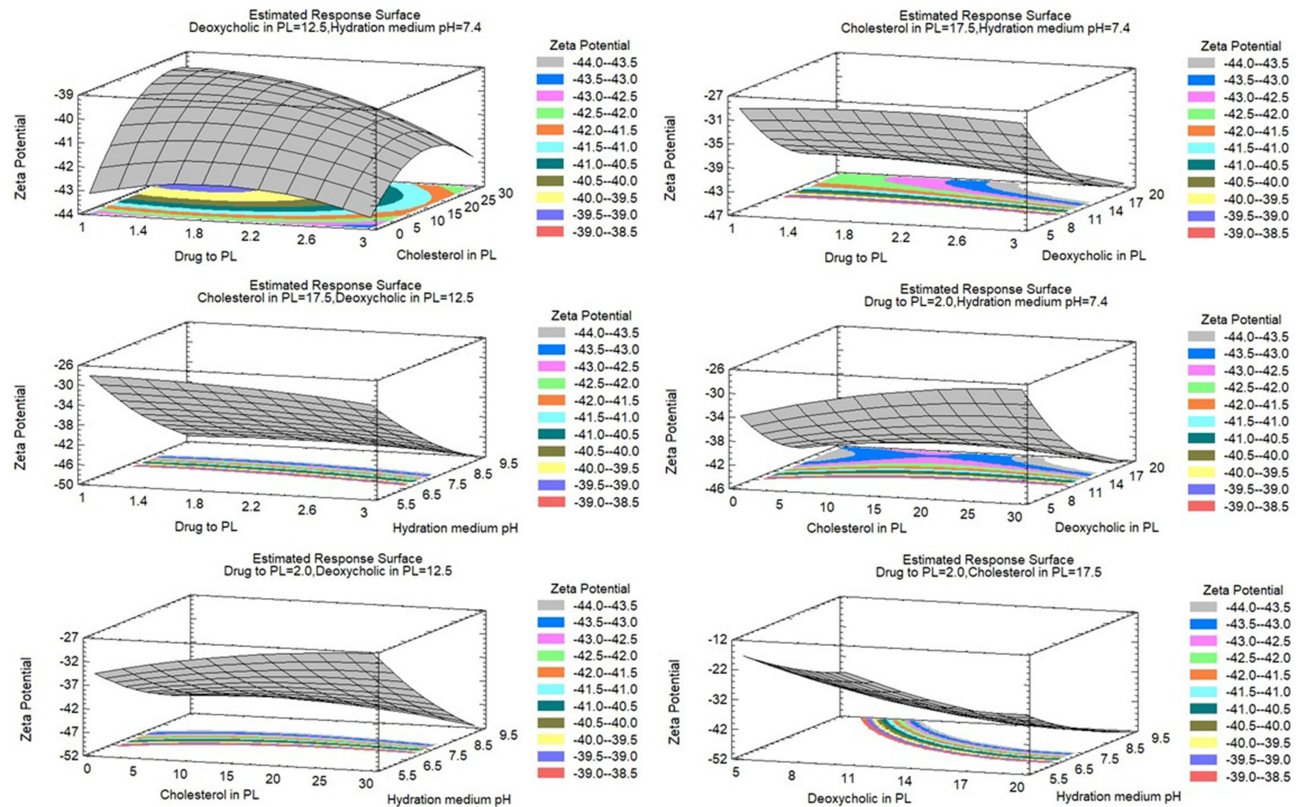


Figure 3 Estimated response surface plots for the effect of the studied factors on zeta potential of the prepared hinokitiol-loaded phytosomal formulations.

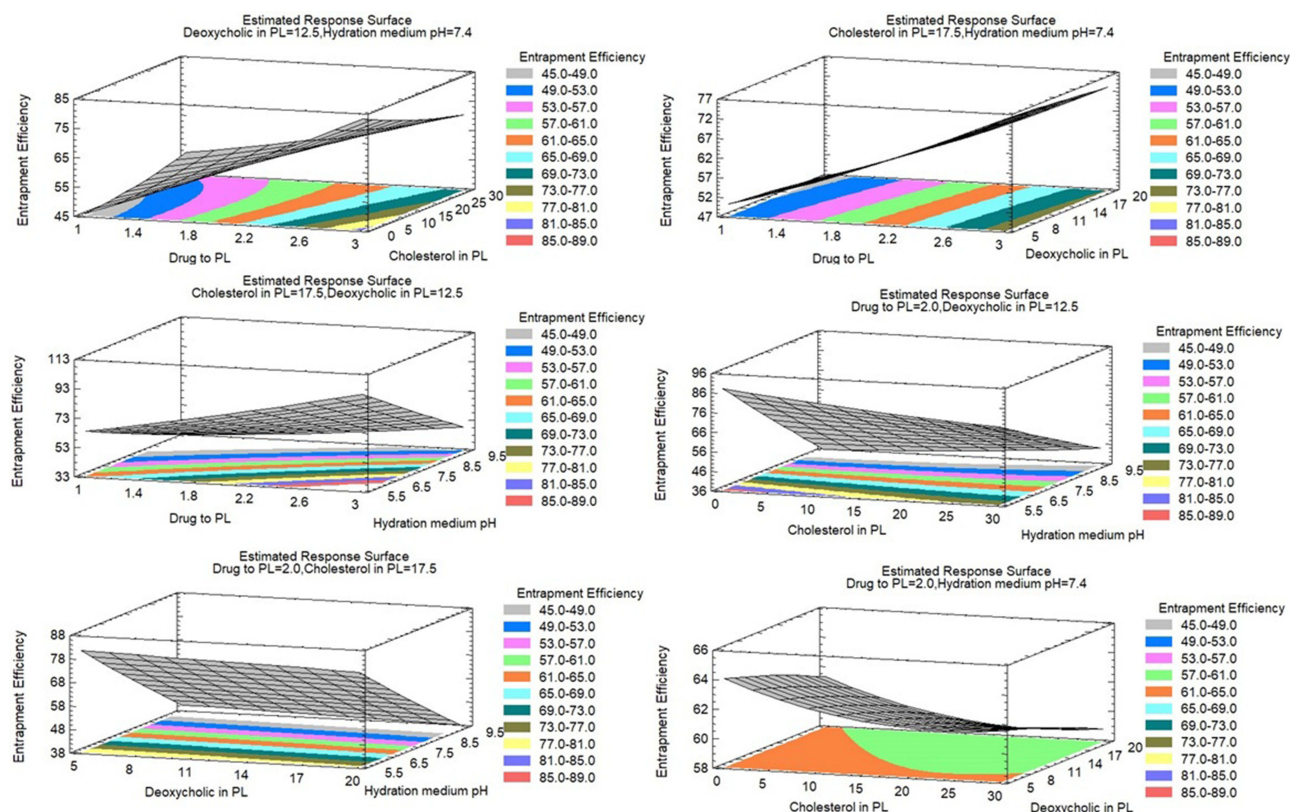


Figure 4 Estimated response surface plots for the effect of the studied factors on entrapment efficiency of the prepared hinokitiol-loaded phytosomal formulations.

the increased cholesterol may promote the formation of multilamellar vesicles, which could further contribute to the observed size increase. The percentage of deoxycholic acid in phospholipid (X3) exhibited an antagonistic effect on particle size and zeta potential. Increasing the amount of deoxycholic acid led to a decrease in both particle size and zeta potential. Deoxycholic acid, known as an anionic surfactant, significantly shifts the zeta potential towards negative values, as previously discussed by Gagliardi et al during the development of sodium deoxycholate-decorated zein nanoparticles.²⁵ As the concentration of deoxycholic acid increases, its amphiphilic properties significantly reduce the surface tension of the medium, particularly at higher surfactant concentrations. This phenomenon facilitates the arrangement of phospholipids into smaller vesicles, as reported previously.²⁶ The pH of the hydration medium exhibited a negative antagonistic effect on both zeta potential and entrapment efficiency. Increasing the pH decreases the zeta potential value, “decreases the negativity”, the impact that could be attributed to adding more alkali upon increasing the pH, and so the particles tend to acquire more negative charge, as previously mentioned.²⁷ Moreover, while it is expected that at higher pH values, the deprotonation of ionizable groups typically leads to an increase in negative surface charge (and therefore a higher zeta potential), in our case, the presence of other components, such as cholesterol and deoxycholic acid, may influence this behavior. These components could shield the surface charge or contribute to changes in the overall surface chemistry of the nanoparticles, leading to a reduction in the magnitude of the zeta potential despite the higher pH. Additionally, in complex systems like phytosomes, the interactions between the lipid bilayer, surfactant, and the surrounding media can influence how the surface charge is distributed. This may result in a non-linear relationship between pH and zeta potential. The effect of the hydration medium pH on the drug entrapment efficiency will be explained later in the hinokitiol solubility study section.

A multiple-response optimization approach was employed to determine the combination of factors that minimize particle size while maximizing zeta potential and drug entrapment efficiency (yielding an overall optimum desirability). This entailed identifying the optimal levels of the independent variables by maximizing a desirability function encompassing the study objectives. The optimized combination of factor levels indicated that the optimal levels for X1, X2, X3, and X4 were 1:3.68 molar ratio, 14.71%, 7.51%, and 4.2, respectively. The predicted values for particle size (Y1), zeta

potential (Y2), and drug entrapment efficiency (Y3) were 138.4 nm, -18.43 mV, and 99.7%, respectively. These predicted values were in excellent agreement with the observed values, with less than 5% residuals.

Morphological Characterization of the Optimized Formulation

The morphological characteristics of the optimized formulation were investigated using optical and transmission electron microscopy (TEM). **Figure 5A and 5B** depict optical microscopy images of the formulation at different magnifications. The formulation exhibits uniformity and spherical morphology at a lower magnification (**Figure 5A**), with no observable aggregation or irregularities. Upon closer examination (**Figure 5B**) at higher magnification, the spherical structure of the particles is more evident, with smooth surfaces indicating well-formed vesicles. This uniformity and spherical morphology indicate a well-prepared formulation with consistent size and shape distribution.

Furthermore, TEM imaging (**Figure 5C**) provided additional insights into the optimized formulation's ultrastructure. The TEM image reveals individual phytosomal nanoparticles with distinct lipid bilayer structures. Multiple layers within the nanoparticles suggest the formation of multilamellar vesicles, which are commonly observed in lipid-based formulations. Additionally, the nanoparticles appear uniformly dispersed without any noticeable aggregation, corroborating the findings from optical microscopy.

The observed morphological characteristics of the optimized formulation align well with the desired attributes for effective drug delivery systems. The uniform spherical shape and well-defined lipid bilayer structure indicate good stability and potential for sustained drug release. The absence of aggregation further suggests that the formulation possesses favorable physical properties essential for optimal drug delivery and therapeutic efficacy. These findings are consistent with previous reports on the morphological characterization of drug-loaded nanoparticles employing similar techniques.^{28–30}

Aqueous Solubility and pH-Dependent Solubility of Hinokitiol

Figure 6 illustrates the solubility of hinokitiol as a function of pH. As depicted, there is a notable increase in the solubility of hinokitiol with increasing pH. Specifically, at lower pH values (4.2 and 5.5), the solubility of hinokitiol is relatively low. However, as the pH of the medium increases, a significant enhancement in solubility is observed, reaching its maximum at alkaline pH values (9.3 and 10.6). This pH-dependent solubility behavior is consistent with the ionization

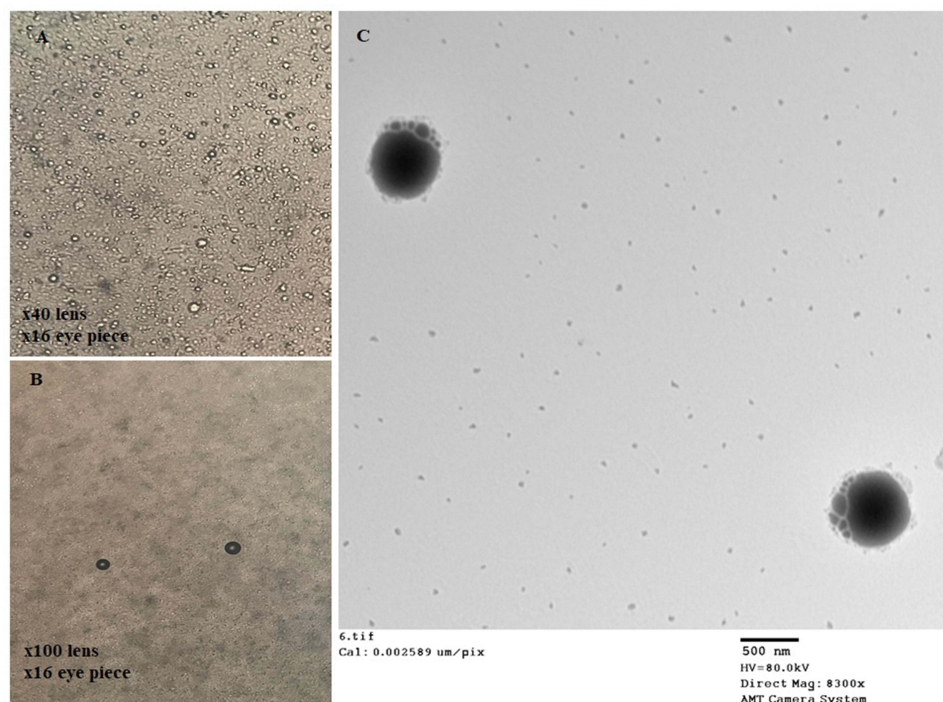


Figure 5 Optical microscope images (**A** and **B**) at two different magnification power, transmission electron microscope micrograph (**C**) for the optimized phytosomal formulation.

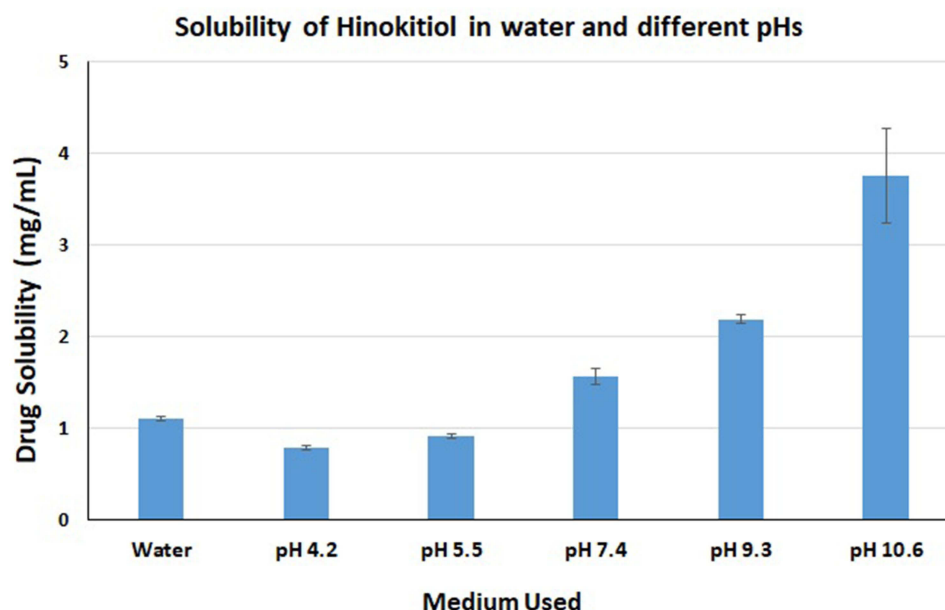


Figure 6 Aqueous hinokitiol solubility and drug solubility at different pHs.

characteristics of hinokitiol, whereby it exists predominantly in its ionized form at higher pH, leading to increased aqueous solubility.

The observed increase in solubility with increasing pH can be attributed to the ionization of hinokitiol molecules, facilitated by the presence of ionizable functional groups. At acidic pH, hinokitiol exists primarily in its unionized form, which has limited solubility in aqueous media. However, as the pH of the medium becomes more alkaline, a greater proportion of hinokitiol molecules ionize, leading to enhanced solubility due to the formation of water-soluble ionized species.

These findings underscore the importance of considering the pH-dependent solubility of hinokitiol in the design of drug delivery systems, particularly for formulations intended for administration via oral or parenteral routes. Moreover, these findings explain the observed decrease in drug entrapment efficiency with an increase in the pH of the hydration medium. This is attributed to the enhanced solubility of the drug in the hydration medium at higher pH levels, resulting in a greater proportion of the drug remaining in the solution rather than being entrapped within the phagosomal formulation.

In vitro Release of Drug-Loaded Optimized Phytosomes

The in vitro release profiles of the drug-loaded optimized phytosomes were evaluated and compared with those of a pure drug suspension. This analysis provides valuable insights into the release behavior of the drug from the phytosomal formulation in a simulated physiological environment. The release of the drug from the optimized phytosomes exhibited a sustained and controlled pattern over time. In contrast, the release profile of the pure drug suspension showed a rapid and complete release of the drug within the initial hours of the experiment. This significant difference in release kinetics highlights the effectiveness of the phytosomal formulation in modulating the release of the drug (data not shown).

The sustained release behavior observed with the phytosomal formulation can be attributed to several factors, including the lipid bilayer structure of the phytosomes, which acts as a barrier to drug diffusion, and the presence of the aqueous core, which facilitates the gradual diffusion of the drug molecules. Additionally, interactions between the drug and the lipid components of the phytosomes may further retard drug release, contributing to the sustained release profile similar finding was reported for the ex vivo permeation of phytosomes, which demonstrated controlled L-carnosine permeation through corneal tissue compared to L-carnosine solution.³¹ Li et al reported that liposomes, as carriers of therapeutic drugs, exhibit controlled drug release properties and attributed this finding to the presence of lipid bilayer structure.³²

The superior performance of the drug-loaded phytosomes in achieving sustained release compared to the pure drug suspension underscores the potential of phytosomal formulations as effective drug delivery systems. By prolonging the

release of the drug and maintaining therapeutic levels over an extended period, phytosomal formulations offer significant advantages in terms of enhanced drug efficacy, reduced dosing frequency, and improved patient compliance.

Assessment of Cell Viability (IC_{50})

Figure 7 depicts the percentage of cell viability of MCF-7 and MDA-MB-231 cells following a 48-hour treatment with various formulations, including hinokitiol phytosomes, cisplatin, pure hinokitiol, and non-medicated phytosomes. Figure 7A shows the cytotoxicity of cisplatin, a commonly used chemotherapy drug, as a reference. Comparisons were made between the cytotoxic effects of hinokitiol phytosomes, pure hinokitiol, and non-medicated phytosomes formulation. The formulation of the hinokitiol phytosomes demonstrated enhanced cytotoxicity against both MCF-7 and MDA-MB-231 breast cancer cells compared to pure hinokitiol and non-medicated phytosomes (Figure 7B and C). Moreover, it was observed that the formulation of the hinokitiol phytosomes exhibited greater cytotoxicity towards MDA-MB-231 cells than MCF-7 breast cancer cell lines (Figure 7B and C).

To quantify the cytotoxicity of hinokitiol phytosomes, IC_{50} values were determined for each cell line. The IC_{50} values represent the concentration of the formulation required to inhibit cell growth by 50%. Using GraphPad Prism software to calculate the IC_{50} , the values for the hinokitiol-loaded phytosome formulation were 18.6 $\mu\text{g}/\text{mL}$ for MCF-7 cells and 5.7 $\mu\text{g}/\text{mL}$ for MDA-MB-231 cells. In comparison, the IC_{50} values of the pure drug for MCF-7 and MDA-MB-231 cells were 39.33 $\mu\text{g}/\text{mL}$ and 8.38 $\mu\text{g}/\text{mL}$, respectively. These results indicate that the formulated hinokitiol in phytosomes exhibits greater anticancer efficacy than the pure hinokitiol. These results underscore the potential of hinokitiol phytosomes as a promising therapeutic agent for breast cancer treatment, with superior cytotoxic activity compared to pure hinokitiol. Cisplatin showed an IC_{50} of 11.36 and 5.2 $\mu\text{g}/\text{mL}$ for MCF-7 cells and MDA-MB-231, respectively.

The findings from this study shed light on the potential of hinokitiol-loaded phytosomal formulations as effective agents against breast cancer. The results demonstrated enhanced cytotoxicity of the formulated phytosomes compared to pure hinokitiol and non-medicated phytosomes, indicating the efficacy of the delivery system in enhancing the therapeutic effects of hinokitiol. The observed cytotoxicity of hinokitiol phytosomes formulation against MCF-7 and MDA-MB-231 breast cancer cells suggests its promising role as a targeted treatment option for breast cancer. The formulation exhibited a dose-dependent cytotoxic effect, with lower IC_{50} values compared to pure hinokitiol, indicating its enhanced potency in inhibiting cancer cell growth. These findings align with previous studies that have reported the anticancer activity of hinokitiol against various cancer cell lines.^{33,34}

The superior cytotoxicity of hinokitiol phytosomal nanoparticles can be attributed to several factors. Firstly, the phytosomal formulation facilitates the efficient delivery of hinokitiol to the cancer cells, ensuring optimal bioavailability and cellular uptake,

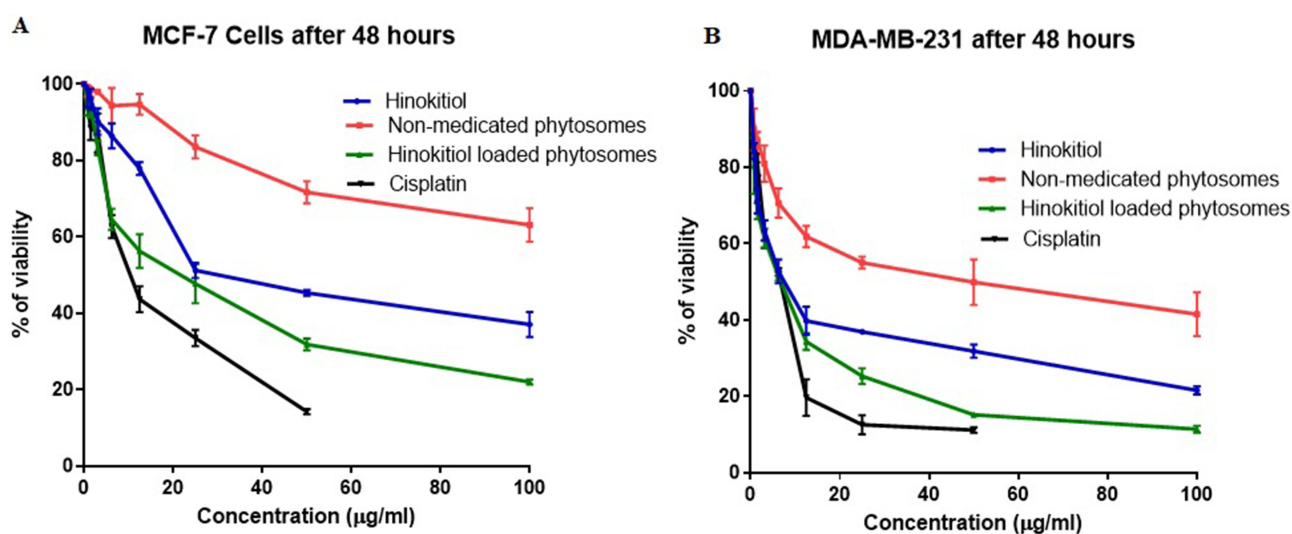


Figure 7 Percentage of cell viability of MCF-7 cells treated with hinokitiol, non-medicated phytosomes, hinokitiol-loaded phytosomes, and cisplatin (A), and cell viability of MDA-MB-231 treated with hinokitiol, non-medicated phytosomes, hinokitiol-loaded phytosomes, and cisplatin (B).

as previously reported for liposomes.³⁵ The lipid bilayer structure of phytosomes protects the encapsulated drug and enables sustained release, prolonging its exposure to cancer cells.³⁶ The differential cytotoxicity observed between MCF-7 and MDA-MB-231 cell lines underscores the importance of considering tumor heterogeneity in breast cancer treatment. The higher sensitivity of MDA-MB-231 cells to hinokitiol phytosomes may be attributed to differences in cellular signaling pathways and molecular characteristics between the two cell lines. Further investigation into the underlying mechanisms responsible for this differential response is warranted to optimize treatment strategies and personalize therapy for individual patients.

Cell Morphology

The assessment of cell morphology provides valuable insights into the effects of treatment on cancer cell behavior and viability. This study evaluated the changes in properties of MDA-MB-231 cells following treatment with different formulations, as depicted in Figure 8. Untreated MDA-MB-231 cells (Figure 8A) displayed typical morphology, characterized by many viable cells with a defined shape and adherence to the culture substrate. Following treatment with cisplatin (Figure 8B), notable changes in the morphology of MDA-MB-231 cells were observed. These changes are indicative of apoptosis commonly induced by cisplatin through DNA damage and activation of apoptotic pathways. Additionally, cisplatin-treated cells exhibited reduced proliferation and altered cytoskeletal organization, contributing to cell shape and mobility changes. Upon treatment with hinokitiol at its IC₅₀ level (Figure 8C), fewer cells and minor morphological changes were observed compared to untreated cells. This reduction in cell number suggests a cytotoxic effect of hinokitiol on MDA-MB-231 cells, leading to decreased cell viability. Interestingly, treatment with hinokitiol formulated in phytosomes (Figure 8D) at its IC₅₀ level resulted in further alterations in cell morphology compared to hinokitiol alone. Changes in cell shape and morphology were evident, along with a decrease in the number of viable cells. Although no noticeable alterations in cell mobility or shaking were observed, the presence of spherical cells,

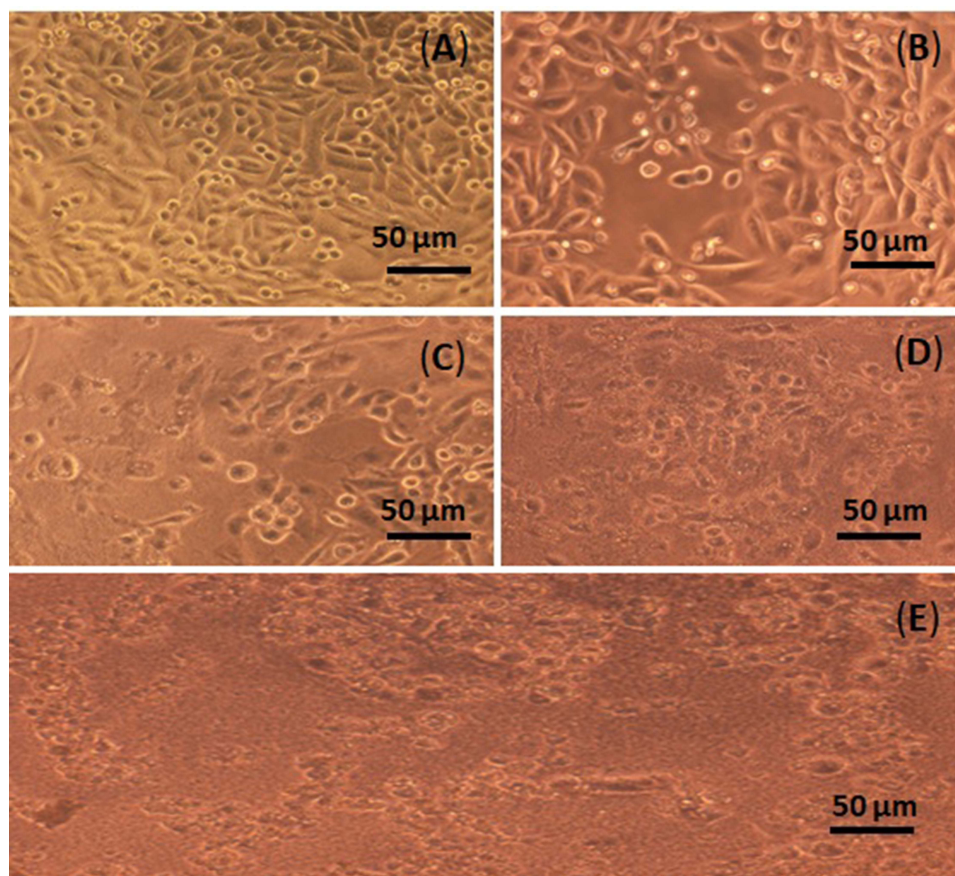


Figure 8 Cell Morphology of the untreated MDA-MB-231 cells (A), cells treated with IC₅₀ of Cisplatin (B), Cells treated with IC₅₀ of hinokitiol (C), Cells treated with IC₅₀ of hinokitiol-loaded phytosomes (D), and cells treated with an equivalent IC₅₀ amount of non-medicated phytosomes (E). At a 20X magnification, every cell was examined.

indicative of cell death, suggests a more pronounced cytotoxic effect of hinokitiol when delivered in phytosomal form. In comparison, treatment with an equivalent IC50 amount of non-medicated phytosomes (Figure 8E) did not induce significant changes in cell morphology, indicating that the observed effects were explicitly attributed to the presence of hinokitiol in the phytosomal formulation.

Overall, the findings suggest that hinokitiol, particularly when formulated in phytosomes, exerts cytotoxic effects on MDA-MB-231 cells, leading to alterations in cell morphology and reduced cell viability. These results underscore the potential of hinokitiol-loaded phytosomal formulations as effective agents for breast cancer treatment, warranting further investigation into their mechanisms of action and therapeutic efficacy in preclinical and clinical settings.

Cell Apoptosis Assay

The study utilized flow cytometry to assess necrosis and apoptosis in MDA-MB-231 breast cancer cells, crucial indicators in evaluating potential anticancer efficacy. Apoptosis, a programmed cell death characterized by DNA damage, was identified by fluorescence staining using Annexin V-FITC and propidium iodide (PI). Annexin V binds to phosphatidylserine exposed on the cell surface during apoptosis, while PI stains the DNA of necrotic or late apoptotic cells.^{37,38}

Figure 9 depicts the percentage of necrotic and apoptotic cells in MDA-MB-231 cells following 24 hours of treatment with pure hinokitiol (Figure 9B), hinokitiol-loaded phytosomal formulation (Figure 9C), and non-medicated phytosomes (Figure 9D). The results obtained were compared to untreated control cells (Figure 9A). Late and early apoptotic cells are represented in the upper and lower right quadrants. The formulation of hinokitiol-loaded phytosomes induced apoptosis in 53% of MDA-MB-231 cells, with 50.8% classified as late apoptotic and 2.6% as early apoptotic (Figure 9C and Table 2). Additionally, 1.9% of cells exhibited necrosis under the influence of the drug-loaded phytosomal formulation.

Comparatively, treatment with pure hinokitiol resulted in lower levels of apoptosis, with 3.8% of cells classified as late apoptotic and 2.7% as necrotic (Figure 9B). Untreated cells exhibited minimal apoptosis or necrosis, with only 0.1% of cells showing signs of either (Figure 9A and Table 2).

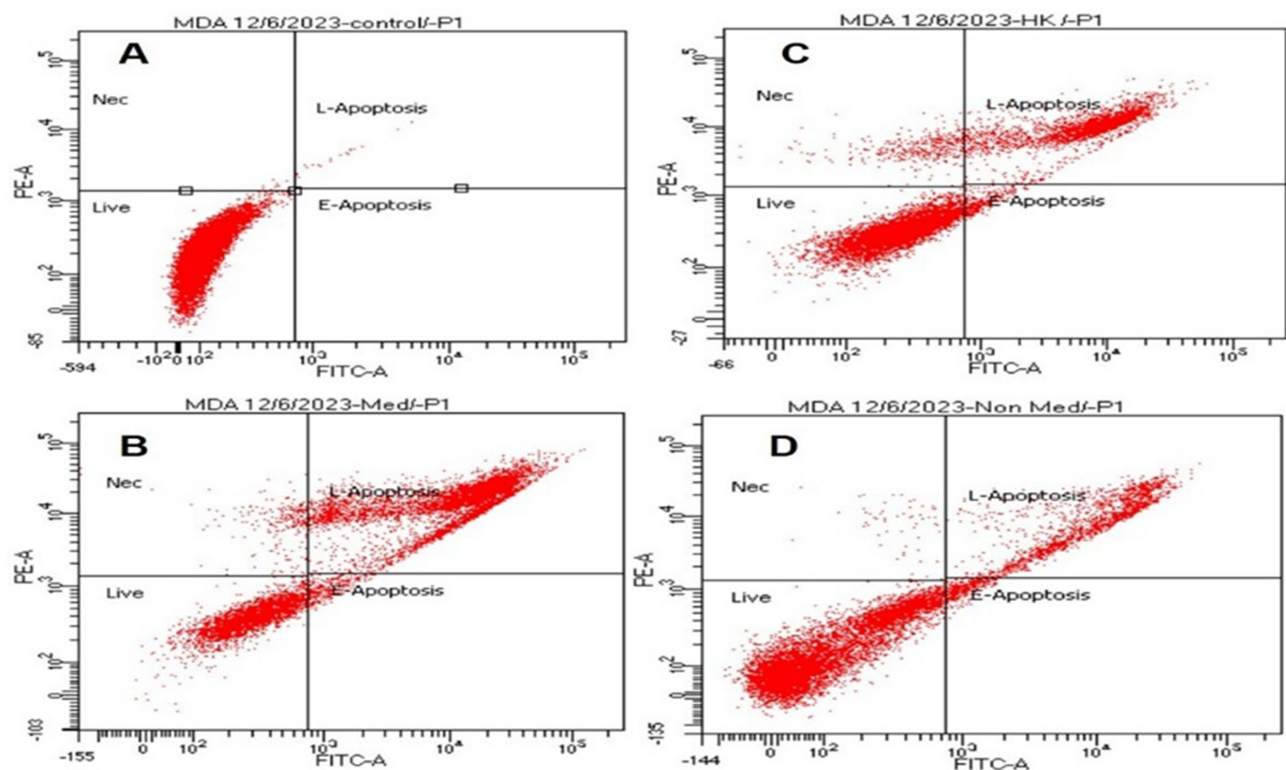


Figure 9 MDA-MB-231 cells staining with Annexin V/PI after 24 hours; control (A); cells treated with pure hinokitiol (B), cells treated with hinokitiol-loaded phytosomal formulation (C), cells treated with non-medicated phytosomes (D).

Notes: % of Viable Cells (Lower left), % of Necrosis (Upper left), % of Early Apoptosis (Lower right), % of Late Apoptosis (Upper right).

Table 2 Percentages of Necrosis and Apoptosis of Cells (Viability and Death) in MDA-MB-231 Cells Treated for 24 hours with IC50 of Pure Hinokitiol, Hinokitiol-Phytosomes, and Non-Medicated Phytosomes

| Treatment | % of Viable Cells | % of Necrosis | % of Early Apoptosis | % of Late Apoptosis |
|--------------------------|-------------------|---------------|----------------------|---------------------|
| Control | 99.9 | 0 | 0 | 0.1 |
| Pure hinokitiol | 66.7 | 4.1 | 3.2 | 26 |
| Hinokitiol-phytosomes | 31.3 | 2.4 | 3.2 | 63.1 |
| Non-medicated phytosomes | 79.7 | 0.6 | 3.7 | 16 |

These findings underscore the efficacy of hinokitiol-loaded phytosomes in inducing apoptosis in MDA-MB-231 breast cancer cells. A higher percentage of apoptotic cells was observed with the phytosomal formulation than with pure hinokitiol, which suggests enhanced therapeutic potential, possibly due to improved drug delivery and bioavailability. These results support further investigation of hinokitiol-loaded phytosomes as a promising strategy for breast cancer therapy.

Cell Cycle Assay

Flow cytometry analysis with propidium iodide (PI) labeling was employed to assess the distribution of MDA-MB-231 cells across the cell cycle phases, including interphase (G0/G1, S, G2) and the mitotic phase (M). The aim was to determine the extent of cell cycle arrest induced by the hinokitiol-loaded phytosomal formulation at specific phases.

Figure 10 illustrates the distribution pattern of MDA-MB-231 cells across the cell cycle phases for normal cells (Figure 10A) and under different treatment conditions (Figure 10B–D). Treatment with the IC50 dosage of hinokitiol-loaded phytosomes resulted in a slight increase in the percentage of cells arrested in the G2/M phase (13%) compared to untreated cells. Furthermore, a higher proportion of cells were observed in the S phase (40.8%) following treatment with

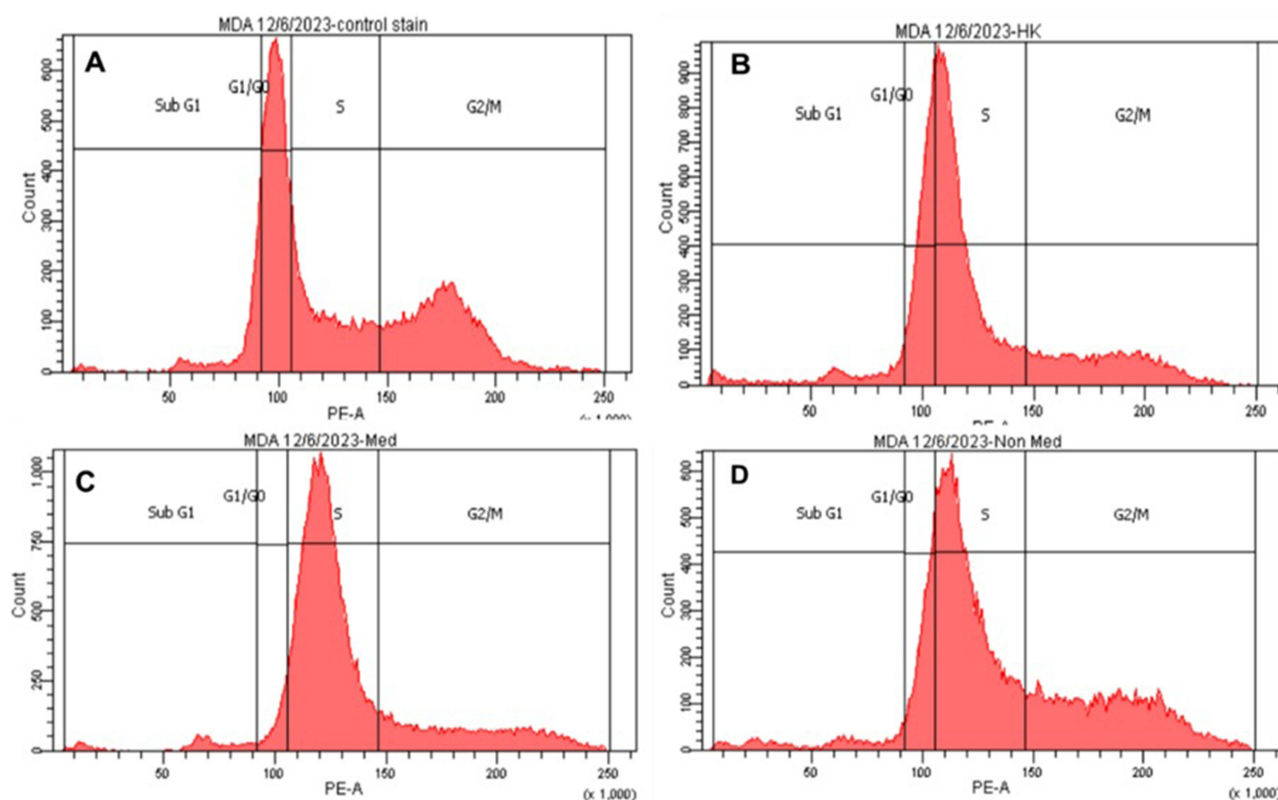


Figure 10 Pattern for the percentage of MDA-MB-231 cells in the cell cycle phases for normal cells (A), cells treated with pure hinokitiol (B), cells treated with hinokitiol-loaded phytosomes, and cells treated with non-medicated phytosomes (D).

Table 3 Percentage of Cells in Different Cell Cycle Phases for Control MDA-MB-231 Cells, Cells Treated with IC50 of Pure Hinokitiol, Cells Treated with IC50 of Drug-Phytosomes, and Cells Treated with Non-Medicated Phytosomes for 24 hours

| Treatment \ Phase | Control | Pure Hinokitiol | Hinokitiol-Loaded Phytosomes | Non-Medicated Phytosomes |
|-------------------|---------|-----------------|------------------------------|--------------------------|
| Sub G1 | 10% | 5.6% | 2.9% | 4.5% |
| G1/G0 | 28% | 16.5% | 2.8% | 10.1% |
| S | 18.5% | 33.4% | 40.8% | 36.6% |
| G2/M | 26.7% | 14.4% | 13% | 23.4% |

the phytosomal formulation. Conversely, there was a decrease in the percentage of cells in the Sub-G1 and G1/G0 phases by 2.9% and 2.8%, respectively, compared to untreated cells.

Specifically, the number of cells treated with hinokitiol-loaded phytosomes decreased by 3.45-fold in the Sub-G1 phase, 10-fold in the G1/G0 phase, and 2-fold in the G2/M phase, while it increased by 2.2 times in the S phase (Figure 10C and Table 3). The percentage of cells in the S phase for pure hinokitiol and formulated hinokitiol phytosomes was 33.4% and 40.8%, respectively.

These findings suggest that the formulation of hinokitiol phytosomes induces cell cycle arrest primarily in the S phase of MDA-MB-231 cells. By arresting cells in the S phase, the phytosomal formulation prevents proliferation and the transmission of damaged DNA to daughter cells,³⁴ thereby inhibiting cancer cell growth. This observation highlights the potential of hinokitiol-loaded phytosomes as a promising strategy for inhibiting cell proliferation and suppressing cancer progression in breast cancer therapy. Further investigations into the molecular mechanisms underlying cell cycle arrest induced by the phytosomal formulation are warranted to elucidate its therapeutic efficacy.

Conclusions

This study demonstrates the potential of hinokitiol-loaded phytosomal formulation as a promising strategy for enhancing the therapeutic efficacy against breast cancer cells. We optimized the formulation to achieve desirable particle size, zeta potential, and drug entrapment efficiency. The optimized formulation exhibited a controlled drug release profile and improved cytotoxicity against MCF-7 and MDA-MB-231 breast cancer cell lines compared to pure hinokitiol and non-medicated phytosomes. Furthermore, our findings highlight the induction of apoptosis and cell cycle arrest, emphasizing the anticancer mechanisms of the formulated hinokitiol. Overall, these results suggest that hinokitiol-loaded phytosomal formulation holds great promise as a potential candidate for developing effective and targeted breast cancer therapeutics. Molecular docking and molecular dynamics simulations warrant a better understanding of the interaction between hinokitiol at the molecular level. Additionally, 3D-printed tablets containing both pure drug and drug-loaded phytosomes have been developed, and their quality control tests, along with in vivo performance evaluations, have been completed. The detailed findings from these studies will be submitted as a separate work, offering further insights into the formulation's performance and therapeutic potential.

Acknowledgments

This research work was funded by Institutional Fund Projects under grant no. (IFPIP: 1733-166-1443). The authors gratefully acknowledge technical and financial support provided by the Ministry of Education and King Abdulaziz University, DSR, Jeddah, Saudi Arabia.

Disclosure

The authors declare no conflict of interest.

References

1. Lukaszewicz S, Czezelewski M, Forma A, Baj J, Sitarz R, Stanislawek A. Breast Cancer—Epidemiology, Risk Factors, Classification, Prognostic Markers, and Current Treatment Strategies—An Updated Review. *Cancers*. 2021;13(17). doi:10.3390/CANCERS13174287
2. Arnold M, Morgan E, Rungay H, et al. Current and future burden of breast cancer: global statistics for 2020 and 2040. *Breast off J Eur Soc Mastol*. 2022;66:15. doi:10.1016/J.BREAST.2022.08.010
3. Sung H, Ferlay J, Siegel RL, et al. Global Cancer Statistics 2020: GLOBOCAN Estimates of Incidence and Mortality Worldwide for 36 Cancers in 185 Countries. *CA Cancer J Clin*. 2021;71(3):209–249. doi:10.3322/CAAC.21660
4. Ali A, Manzoor MF, Ahmad N, et al. The Burden of Cancer, Government Strategic Policies, and Challenges in Pakistan: a Comprehensive Review. *Front Nutr*. 2022;9:940514. doi:10.3389/FNUT.2022.940514
5. Ghose S, Radhakrishnan V, Bhattacharya S. Ethics of cancer care: beyond biology and medicine. *Ecancermedicalscience*. 2019;13. doi:10.3332/ECANCER.2019.911
6. Aryan H. The Role of Herbal Medicine as Anti-Cancer Medicine: from the Claim to Truth. *Galen Med J*. 2018;7:e1179. doi:10.22086/GMJ.V0I0.1179
7. Ali M, Wani SUD, Salahuddin M, et al. Recent advance of herbal medicines in cancer- a molecular approach. *Heliyon*. 2023;9(2):1. doi:10.1016/J.HELIYON.2023.E13684
8. Sorrenti V, Burò I, Consoli V, Vanella L. Recent Advances in Health Benefits of Bioactive Compounds from Food Wastes and By-Products: biochemical Aspects. *Int J Mol Sci*. 2023;24(3):2019. doi:10.3390/IJMS24032019
9. Tavakoli J, Mir S, Zadehzare MM, Akbari H. Evaluation of Effectiveness of Herbal Medication in Cancer Care: a Review Study. *Iran J Cancer Prev*. 2012;5(3):144.
10. Charana Sriya K, Sai D, Ravi Sankar P. Phytosomes: a Novel Approach for Herbal Phytochemicals for Enhancing the Bioavailability. *Int J Pharm Sci Rev Res*. 2020;60:21–26.
11. Karimi N, Ghanbarzadeh B, Hamishehkar H, Keivani F, Pezeshki A, Gholian MM. Phytosome and Liposome: the Beneficial Encapsulation Systems in Drug Delivery and Food Application. *Appl Food Biotechnol*. 2015;2(3):17–27. doi:10.22037/afb.v2i3.8832
12. Jamal A, Asseri AH, Ali EMM, et al. Preparation of 6-Mercaptopurine Loaded Liposomal Formulation for Enhanced Cytotoxic Response in Cancer Cells. *Nanomaterials*. 2022;12(22):1–14. doi:10.3390/nano12224029
13. Ahmed TA. Preparation of transfersomes encapsulating sildenafil aimed for transdermal drug delivery: plackett–Burman design and characterization. *J Liposome Res*. 2015;25(1):1–10. doi:10.3109/08982104.2014.950276
14. Ahmed TA. Study the pharmacokinetics, pharmacodynamics and hepatoprotective activity of rosuvastatin from drug loaded lyophilized orodispersible tablets containing transfersomes nanoparticles. *J Drug Deliv Sci Technol*. 2021;63:102489. doi:10.1016/j.jddst.2021.102489
15. Ali EMM, Elashkar AA, El-Kassas HY, Salim EI. Methotrexate loaded on magnetite iron nanoparticles coated with chitosan: biosynthesis, characterization, and impact on human breast cancer MCF-7 cell line. *Int J Biol Macromol*. 2018;120(Pt A):1170–1180. doi:10.1016/J.IJBIOMAC.2018.08.118
16. van Meerloo J, Kaspers GJL, Cloos J. Cell sensitivity assays: the MTT assay. *Methods Mol Biol*. 2011;731:237–245. doi:10.1007/978-1-61779-080-5_20
17. Jan R, Chaudhry GS. Understanding Apoptosis and Apoptotic Pathways Targeted Cancer Therapeutics. *Adv Pharm Bull*. 2019;9(2):205. doi:10.15171/APB.2019.024
18. Elmore S. Apoptosis: a Review of Programmed Cell Death. *Toxicol Pathol*. 2007;35(4):495. doi:10.1080/01926230701320337
19. Rieger AM, Nelson KL, Konowalchuk JD, Barreda DR. Modified annexin V/propidium iodide apoptosis assay for accurate assessment of cell death. *J Vis Exp*. 2011;50:3–6.
20. Maes A, Menu E, de Veirman K, Maes K, Vanderkerken K, de Bruyne E. The therapeutic potential of cell cycle targeting in multiple myeloma. *Oncotarget*. 2017;8(52):90501. doi:10.18632/ONCOTARGET.18765
21. Ligasová A, Frydrych I, Koberna K. Basic Methods of Cell Cycle Analysis. *Int J Mol Sci*. 2023;24(4):3674. doi:10.3390/IJMS24043674
22. Fried J, Perez AG, Clarkson BD. Flow cytometric analysis of cell cycle distributions using propidium iodide: properties of the method and mathematical analysis of the data. *J Cell Biol*. 1976;71(1):172–181. doi:10.1083/JCB.71.1.172
23. Nakhaei P, Margiana R, Bokov DO, et al. Liposomes: structure, Biomedical Applications, and Stability Parameters With Emphasis on Cholesterol. *Front Bioeng Biotechnol*. 2021;9:705886. doi:10.3389/FBIOE.2021.705886
24. Tefas LR, Sylvester B, Tomuta I, et al. Development of antiproliferative long-circulating liposomes co-encapsulating doxorubicin and curcumin, through the use of a quality-by-design approach. *Drug Des Devel Ther*. 2017;11:1605–1621. doi:10.2147/DDDT.S129008
25. Gagliardi A, Paolino D, Iannone M, Palma E, Fresta M, Cosco D. Sodium deoxycholate-decorated zein nanoparticles for a stable colloidal drug delivery system. *Int J Nanomed*. 2018;13:601–614. doi:10.2147/IJN.S156930
26. Ahmed TA. Development of rosuvastatin flexible lipid-based nanoparticles: promising nanocarriers for improving intestinal cells cytotoxicity. *BMC Pharmacol Toxicol*. 2020;21(1). doi:10.1186/s40360-020-0393-8
27. Malvern Ltd. Zeta potential: an Introduction in 30 minutes. 2011. Available from: <http://scholar.google.com/scholar?hl=en&btnG=Search&q=intitle:Zeta+Potential+An+Introduction+in+30+Minutes#0>. Accessed October 10, 2024.
28. Ahmed TA, El-Say KM, Aljaeid BM, Fahmy UA, Abd-Allah FI. Transdermal glimepiride delivery system based on optimized ethosomal nano-vesicles: preparation, characterization, in vitro, ex vivo and clinical evaluation. *Int J Pharm*. 2016;500(1–2):245–254. doi:10.1016/j.ijpharm.2016.01.017
29. Rodrigues S, Cordeiro C, Seijo B, Remuñán-López C, Grenha A. Hybrid nanosystems based on natural polymers as protein carriers for respiratory delivery: stability and toxicological evaluation. *Carbohydr Polym*. 2015;123:369–380. doi:10.1016/j.carbpol.2015.01.048
30. El-Say KM, Alamri SH, Alsulimani HH, et al. Incorporating valsartan in sesame oil enriched self-nanoemulsifying system-loaded liquisolid tablets to improve its bioavailability. *Int J Pharm*. 2023;639:122966. doi:10.1016/j.ijpharm.2023.122966
31. Abdelkader H, Longman MR, Alany RG, Pierscionek B. Phytosome-hyaluronic acid systems for ocular delivery of L-carnosine. *Int J Nanomed*. 2016;11:2815. doi:10.2147/IJN.S104774
32. Li J, Wang X, Zhang T, et al. A review on phospholipids and their main applications in drug delivery systems. *Asian J Pharm Sci*. 2015;10(2):81–98. doi:10.1016/J.AJPS.2014.09.004

33. Hachlafi NE, Lakhdar F, Khouchlaa A, et al. Health benefits and pharmacological properties of hinokitiol. *Processes*. 2021;9(9):1–21. doi:10.3390/pr9091680
34. Li LH, Wu P, Lee JY, et al. Hinokitiol induces DNA damage and autophagy followed by cell cycle arrest and senescence in gefitinib-resistant lung adenocarcinoma cells. *PLoS One*. 2014;9(8):e104203. doi:10.1371/journal.pone.0104203
35. He H, Lu Y, Qi J, Zhu Q, Chen Z, Wu W. Adapting liposomes for oral drug delivery. *Acta Pharm Sin B*. 2019;9(1):36–48. doi:10.1016/j.apsb.2018.06.005
36. Sabit H, Abdel-Hakeem M, Shoala T, et al. Nanocarriers: a Reliable Tool for the Delivery of Anticancer Drugs. *Pharmaceutics*. 2022;14(8):1566. doi:10.3390/PHARMACEUTICS14081566
37. Kari S, Subramanian K, Altomonte IA, Murugesan A, Yli-Harja O, Kandhavelu M. Programmed cell death detection methods: a systematic review and a categorical comparison. *Apoptosis*. 2022;27(7):482–508. doi:10.1007/S10495-022-01735-Y
38. Wlodkowic D, Telford W, Skommer J, Darzynkiewicz Z. Apoptosis and Beyond: cytometry in Studies of Programmed Cell Death. *Methods Cell Biol*. 2011;103:55. doi:10.1016/B978-0-12-385493-3.00004-8

International Journal of Nanomedicine

Dovepress

Publish your work in this journal

The International Journal of Nanomedicine is an international, peer-reviewed journal focusing on the application of nanotechnology in diagnostics, therapeutics, and drug delivery systems throughout the biomedical field. This journal is indexed on PubMed Central, MedLine, CAS, SciSearch®, Current Contents®/Clinical Medicine, Journal Citation Reports/Science Edition, EMBase, Scopus and the Elsevier Bibliographic databases. The manuscript management system is completely online and includes a very quick and fair peer-review system, which is all easy to use. Visit <http://www.dovepress.com/testimonials.php> to read real quotes from published authors.

Submit your manuscript here: <https://www.dovepress.com/international-journal-of-nanomedicine-journal>